Chapter 1

Introduction

- Problem statement
- Opportunity of voltage imaging, core idea of inverting the causal 'presynaptic spike → postsynaptic PSP' relation
- Overview of thesis

1.1 Connectomics

- Motivation
- Ground-truth connectomics: tracing of electron microscopy and fluoresent injection imaging
- Necessity of connection *inference*
- Mention 'invasive' connection testing (stimulate one cell, record possible neighbours)
- Limitations of 'connectomics', and of inferred vs 'actual' connectomics.
  Terminology, e.g. 'functional connectomics'

1.2 Voltage imaging

- Technologies (from dyes to GEVIs)
- Specs: cell yield, tissue depth, recording duration, SNR, species
- ..and growth of these over time, and comparison with calcium imaging.
  To extrapolate how these might advance in the future
- Comparison with other recording techniques: ephys, calcium imaging, (and briefly mention coarser methods)

1.3 Network inference

- Working with events/spikes only, versus working with continuous signals; or a hybrid as here.
- Overview of the spikes-only methods
- The connectomics competition, and the findings about the best methods
- Mention other application domains, like gene regulatory networks
- Conclusion: connection inference by spikes is poor (Ila Fiete etc), and Vm imaging offers unique advantage (causality)

Chapter 2

Simulation details

In this chapter, we decribe our experimental setup: the neuron model we simulate, its inputs, and how we simulate voltage imaging.

2.1 The AdEx neuron model

We choose to simulate the 'AdEx' neuron model, or the 'adaptive exponential integrate-and-fire' neuron.[BG05] This is a leaky-integrate-and-fire (LIF) neuron model, with two additions. First, the full upstroke of each spike is simulated, as an exponential runoff. Second, an extra dynamic variable is added: the adaptation current. This current allows the simulation of many non-linear effects of real neurons, like spike-rate adaptation and post-inhibitory rebound.

The AdEx model consists of two differential equations, one to simulate the membrane voltage V, and one for the adaptation current w:

$$C\frac{\mathrm{d}V}{\mathrm{d}t} = -g_L(V - E_L) + g_L\Delta_T \exp\left(\frac{V - V_T}{\Delta_T}\right) - I_{\text{syn}} - w \quad (1)$$

$$\tau_w\frac{\mathrm{d}w}{\mathrm{d}t} = a(V - E_L) - w \quad (2)$$

I_{syn} is the synaptic current, explained in section 2.4. We use the sign convention of inter alia Dayan & Abbott[1] where membrane currents are defined as positive when positive charges flow *out* of the cell. I.e. a positive I_{syn} decreases the membrane voltage (itself defined as the electric potential inside minus outside the cell).

Other parameters are explained in table 2.1.

In this chapter, we will often analyse $\frac{\mathrm{d}V}{\mathrm{d}t}$ as a function of V, i.e. analyse it as a dynamical system: will the voltage increase or decrease at the current voltage? For conciceness, we will call this function $F(V)$. I.e. $F(V) = \frac{\mathrm{d}V}{\mathrm{d}t}$ = the right-hand-side of equation (1) here, scaled by $1/C$. We'll mostly analyse F in the absence of synaptic and adaptation currents, i.e. for I_{syn} and w both zero. Figure 1 shows the $F(V)$ curve for an AdEx neuron fit to a real neuron.

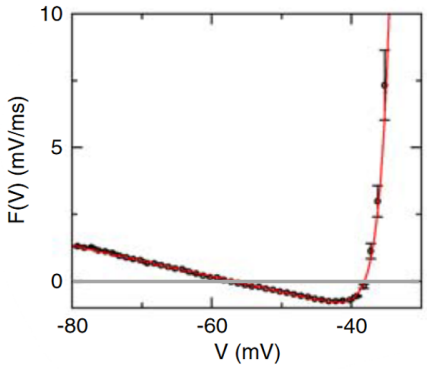

Figure 1: A linear-plus-exponential model (red) fit to data from a cortical pyramidal neuron (black), from [Bad+08]

[1] [DA01], ch. 5.3, p. 162

Name	Description	Value
V	Membrane voltage	(in mV)
w	Adaptation current	(in pA)
C	Membrane capacitance	104 pF
g_L	Input / leak conductance	4.3 nS
E_L	Resting / leak potential	−65 mV
Δ_T	Threshold slope factor	0.8 mV
V_T	Location of minimum of $\frac{\mathrm{d}V}{\mathrm{d}t}$	−52 mV
τ_w	Time constant of adaptation current	88 ms
a	Sensitivity of adaptation current to V	−0.8 nS
θ	Spike definition threshold	40 mV
V_r	Reset voltage after spike	−53 mV
b	Adaptation current bump after spike	65 pA

Table 2.1: Quantities and parameters of the AdEx neuron, equations (1) to (3). Values are from a model fit to a cortical regular spiking (RS) neuron, from [Nau+08]. By defining the location of $\frac{\mathrm{d}V}{\mathrm{d}t}$'s minimum, V_T also determines the location of the firing threshold.

We solve these equations using first-order (Euler) integration, with a timestep Δt of 0.1 ms.

In addition to the two differential equations, the AdEx model also consists of an instantaneous reset condition. When the membrane voltage V reaches a certain threshold θ, a spike is recorded, V is reset, and w is increased:

$$\text{if } V > \theta \text{ then: } \begin{aligned} V &\leftarrow V_r \\ w &\leftarrow w + b \end{aligned} \tag{3}$$

We choose to simulate a cortical regular spiking (RS) neuron, i.e. a 'standard' excitatory neuron that does not display e.g. bursting or fast-spiking behaviour. We take our parameter values from [Nau+08][2], where they fitted an AdEx model to recordings from real cortical RS neurons injected with different step currents.

[2] Section 6, and Table 1, row 3

Analysis

Where are the fixed points of the dynamical system $\frac{\mathrm{d}V}{\mathrm{d}t} = F(V)$? I.e, where is $F = 0$? Like other neuron models, there are two fixed points: a stable one at the leak potential E_L, and an unstable one at the instantaneous firing threshold (which we'll call E_T).

We see in equation (1) (for $I_{\text{syn}} = 0$ and $w = 0$) that the leak potential E_L is indeed a fixed point – or rather lies very close to one: the exponential term is negligibly small at $V = E_L$. The second fixed point has no straightforward expression. The exact solutions for F's roots need the so called Lambert W or 'product logarithm' functions W_0 and W_{-1} (see figure 2). The roots are found at:

$$V = E_L - \Delta_T W_k \left(-\exp\left(\frac{E_L - V_T}{\Delta_T} \right) \right) \tag{4}$$

..where $k = 0$ gives the resting potential, and $k = -1$ the instantaneous firing threshold.[3] For our cortical RS neuron, this gives us an

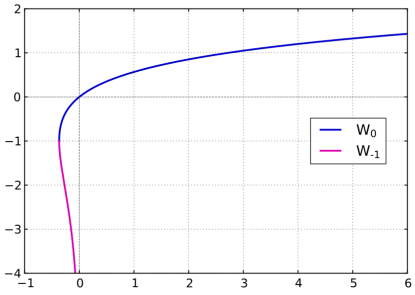

Figure 2: The Lambert W functions for real numbers.

[3] Here too we see that the true resting potential is almost identical to E_L: W_0 passes through zero, and its argument is ≈ 0, because the exponential's argument is negative. For W_{-1} however, figure 2 shows that the second term is not negligible around 0.

instantaneous threshold of $E_T = -49.6$ mV.

Also of interest – especially when comparing with the Izhikevich neuron later – is the slope of AdEx's $F(V)$, i.e. its derivative with respect to V:

$$\begin{aligned}\frac{\mathrm{d}F}{\mathrm{d}V} &= \frac{\mathrm{d}}{\mathrm{d}V}\left(-g_L(V-E_L) + g_L\Delta_T \exp\left(\frac{V-V_T}{\Delta_T}\right)\right) \\ &= -g_L + g_L\Delta_T\frac{1}{\Delta_T}\exp\left(\frac{V-V_T}{\Delta_T}\right) \end{aligned} \tag{5}$$

This derivative is zero at $V = V_T$. I.e, unlike what is suggested by the 'T' subscript, and the name 'effective threshold potential' given to it in the AdEx literature[BG05; Nau+08], V_T is not the instantaneous threshold potential (it is not a zero of F), but rather the minimum of F (it is the zero of $\frac{\mathrm{d}F}{\mathrm{d}V}$).

From equation (5), we also calculate the slope of F at its two roots. At $V = E_L$, the slope (also known as the leak or input conductance here) is $-g_L$, plus a negligibly small exponential term. The negative sign shows that this is a stable fixed point: in a linearization of F around this point, at voltages below the resting potential, F (i.e. $\frac{\mathrm{d}V}{\mathrm{d}t}$) is positive and thus V will increase. At voltages above E_L, F is negative and V will decrease. Small deviations on either side of the resting potential will thus decay back to this resting potential.

At the firing threshold $V = E_T$ (i.e. the second solution to equation (4)), the slope is:

$$g_L\left(\exp\left(\frac{E_T - V_T}{\Delta_T}\right) - 1\right) \tag{6}$$

..which is positive (as $E_T > V_T$), indicating that this is an unstable fixed point: a small deviation of the voltage above E_T will blow up to infinity (i.e, a spike is generated).

2.2 Alternative neuron models

Why did we choose the AdEx model to simulate neuron voltages? In short, because it strikes a good balance between realism and complexity. We briefly consider here two alternative neuron models: the simple leaky-integrate-and-fire (LIF) neuron, and the more complex Hodgkin-Huxley (HH) neuron. In the next section, we go into more depth on a third alternative, the very similar Izhikevich neuron.

A simpler model than AdEx would be the well-known LIF neuron:

$$C\frac{\mathrm{d}V}{\mathrm{d}t} = -g_L(V - E_L) - I_{\text{syn}}$$

$$\text{if } V > \theta, \text{ then: } V \leftarrow V_r$$

As is apparent from comparing this with equations (1) and (3), the AdEx model is an extension of the LIF model. The LIF neuron lacks

a simulation of the upstroke of spikes (the exponential term in equation (1)), and the slower time-scale adaptation current (equation (2)), which allows the simulation of many qualitatively different real neuron types. It is especially this first addition, the full upstroke simulation, that seems relevant in generating realistic voltage traces.

Would this thesis have been very different had we used LIF neurons instead? Probably not, though it might depend on the mean voltage level of the simulated neuron: if it is well below the firing threshold, both LIF and AdEx are linear (the exponential term is negligible), and they behave quasi identically. When a spike is generated in the AdEx model, the exponential feedback makes the upstroke very fast, and thus not many timesteps in the simulation are spent on it, versus the linear regime.

On the other hand, when the neuron would continuously teeter just below its firing threshold, the LIF and AdEx models do not behave similarly. LIF's $F(V)$ curve is still fully linear, while AdEx's is not, and AdEx will behave more like a real neuron – see figure 1.

Another well-known alternative neuron model is the class of Hodgin-Huxley (HH)-like neurons. These models simulate the full trajectory of a spike: both its upstroke and its downstroke. Unfortunately they also have many free parameters. They also take a bit longer to simulate, being higher dimensional (having more differential equations), and containing many more exponential terms, which take the brunt of the time when numerically evaluating a differential expression.

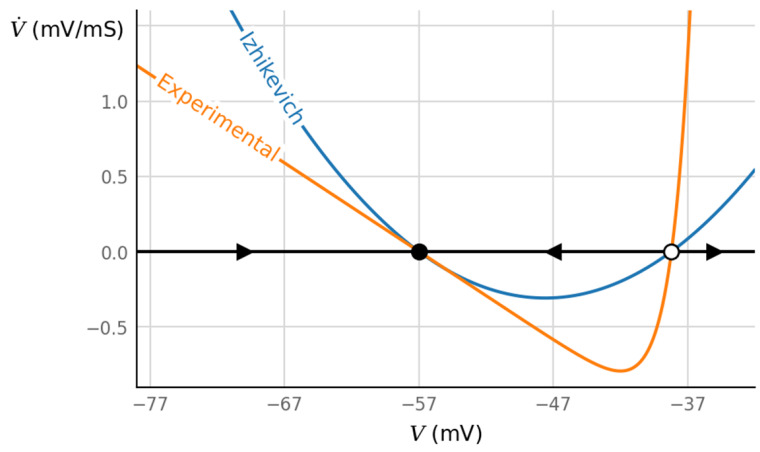

Figure 3: Neuron models as dynamical systems: a comparison of the $F(V)$ curves of the Izhikevich and AdEx neurons. 'Experimental' is an AdEx neuron fit to a cortical pyramidal neuron (using data from [Bad+08]). The Izhikevich neuron's parameters were chosen to match the fixed points and the leak conductance. Arrows indicate whether the voltage will increase or decrease (1D flow field). $\rightarrow \bullet \leftarrow$ is a stable fixed point (resting potential), $\leftarrow \circ \rightarrow$ is an unstable fixed point (spike threshold). $\dot{V} \equiv \frac{\mathrm{d}V}{\mathrm{d}t}$.

2.3 The Izhikevich neuron

Another alternative neuron model is the Izhikevich neuron, which is exceedingly similar to the AdEx neuron. These are the Izhikevich equations, using the same symbols as used before (in equations (1) to (3)):

$$C\frac{\mathrm{d}V}{\mathrm{d}t} = k(V - E_L)(V - E_T) - I_{\text{syn}} - w \tag{7}$$

$$\tau_w \frac{\mathrm{d}w}{\mathrm{d}t} = a(V - E_L) - w \tag{8}$$

$$\begin{aligned} &\text{if } V > \theta, \text{ then:} \\ &\quad V \leftarrow V_r \\ &\quad w \leftarrow w + \Delta w \end{aligned} \tag{9}$$

We have introduced two new parameters not present in the AdEx equations: the steepness of the parabola, k; and E_T, the instantaneous firing threshold (the firing threshold in the absence of any synaptic or adaptation currents).

The only difference with AdEx is in equation (7), where the $F(V)$ curve is not made by a linear plus exponential term, as in AdEx; but rather by a quadratic (a parabola). Its two zeros (the fixed points) are readily apparent, as E_L and E_T.

Correspondences with AdEx

In Izhikevich's book[4], different names are used for the same quanti-

[4] [Izh07], section 5.2.4, equations 5.7 & 5.8

ties:

$$C\frac{\mathrm{d}v}{\mathrm{d}t} = k(v - v_r)(v - v_t) - u + I \tag{10}$$

$$\frac{\mathrm{d}u}{\mathrm{d}t} = a(b(v - v_r) - u) \tag{11}$$

$$\begin{aligned} &\text{if } v > v_{\text{peak}}, \text{ then:} \\ &v \leftarrow c \\ &u \leftarrow u + d \end{aligned} \tag{12}$$

Table 2.2 compares both notation conventions.

AdEx	Izh	Description	Units
V	v	Membrane voltage	V
w	u	Adaptation current	A
τ_w	$1/a$	Time constant of adaptation current	s
E_L	v_r	Resting / leak potential	V
V_r	c	Reset voltage after spike	V
a	b	Sensitivity of adapt. current to V	S
b	d	Adaptation current bump after spike	A

Table 2.2: Different symbols used for the same quantities in [BG05] ('AdEx') and [Izh07] ('Izh'). Membrane capacitance C (in farad) is the same in both notations.

Beside these straightforward correspondences, there are some parameters in either model that have no direct equivalent in the other: k and v_t in Izhikevich, and g_L, Δ_T, and V_T in AdEx. For those, we'll look at the shape of Izhikevich's $F(V)$, as we've done for the AdEx neuron before.

First, the AdEx parameter g_L. This is the input conductance, a.k.a. the leak conductance, and the slope of $F(V)$ around the leak potential. We can find this same conductance for the Izhikevich neuron by taking the derivative with respect to v of the right hand side of equation (10), at $w = 0$, $I_{\text{syn}} = 0$, and $v = v_r$. We find:

$$\frac{\mathrm{d}}{\mathrm{d}v}(k(v - v_r)(v - v_t))\Big|_{v=v_r} = k(v_r - v_t) \tag{13}$$

(this value is negative: the leak potential is a stable fixed point. This corresponds to equation (1), where we find '$-g_L$'). Thus, our first nontrivial correspondence:

$$g_L = k(v_t - v_r) \tag{14}$$

We've seen that V_T is the minimum of AdEx's F. The minimum of Izhikevich's F is easily found as the average of the parabola's two zeros. I.e, V_T corresponds to $(v_r + v_t)/2$.

Finally, Δ_T co-determines the slope of AdEx's F at the firing threshold (equation (6)). Given that Izhikevich's F is a parabola, with slopes equal in magnitude at both roots, we already know the firing

threshold slope: it is the same as the leak conductance, equation (14). Here, the AdEx model is more expressive than Izhikevich's: the slope of $\frac{\mathrm{d}V}{\mathrm{d}t}$ at the firing threshold can be independently tweaked from the leak conductance; in Izhikevich these two are clung together by the form of the quadratic equation.

Comparison with AdEx

The Izhikevich and AdEx models are very similar. Their phase spaces are topologically identical: the adaptive current equation is identical (up to a renaming of the variables); and the $F(V)$-graph has the same shape, with two fixed points: a stable fixed point at the resting potential, and an unstable one at the firing threshold (figure 3).

They differ in the exact shape: Izhikevich's $F(V)$ is a parabola, while AdEx is the more realistic 'linear subthreshold, and then transitioning to an exponential' (see figures 1 and 3). As a result, Izhikevich neurons have an unrealistically slow spike upstroke, examples of which can be seen in figure 4.

A second issue is Izhikevich's subthreshold nonlinearity. The effects of this can be seen in figure 5. Positive input currents produce stronger responses than equally large negative input currents. This is explained by the quadratic $\frac{\mathrm{d}V}{\mathrm{d}t}$ shape: positive deviations are attenuated less, and negative deviations more, than a linear neuron

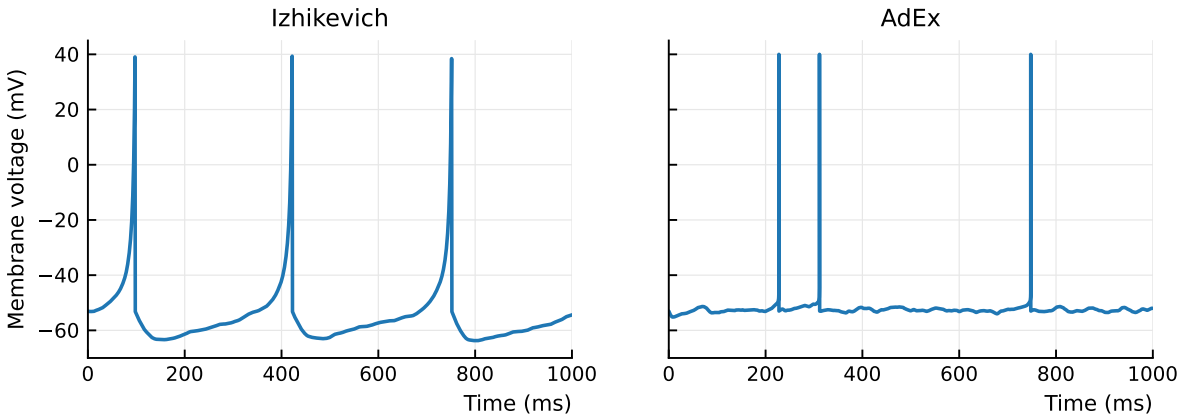

Figure 4: **Two neuron models behave differently for (near) identical parameters and input.**
The AdEx neuron's parameters are from [Nau+08], for a cortical regular spiking neuron. The Izhikevich neuron's parameters are copied from the AdEx neuron wherever they correspond directly. The other parameters are chosen so both models have the same resting and threshold potentials, and the same leak conductance, using the correspondences found earlier in this section. Both models receive EI-balanced synaptic input from 6500 Poisson spike trains with lognormal firing rates. The AdEx neuron was given stronger inputs ($\Delta g_{\text{exc}} = 14$ pS) than the Izhikevich neuron ($\Delta g_{\text{exc}} = 5$ pS), so as to obtain the same number of output spikes. (In both cases, $\Delta g_{\text{inh}} = 4\ \Delta g_{\text{exc}}$). See https://tfiers.github.io/phd/nb/2023-06-23__Vm_traces_AdEx_Izh__Brian.html for more details.

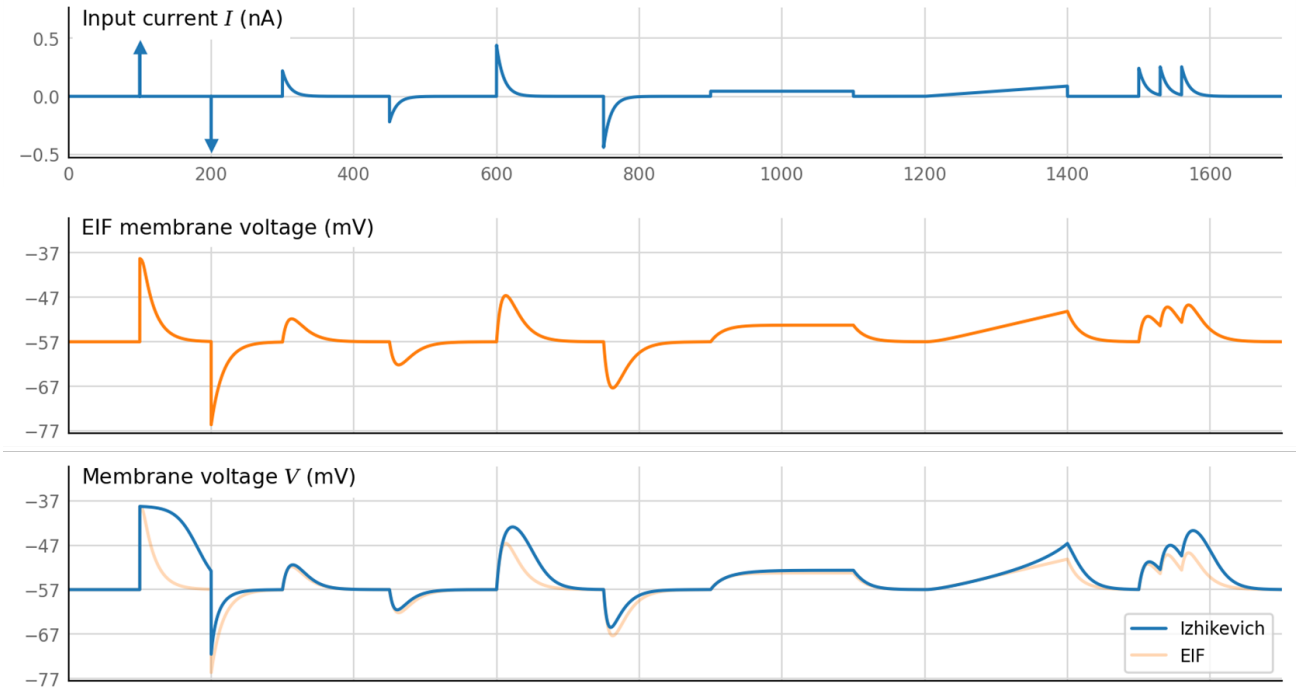

Figure 5: **The nonlinear response of Izhikevich neurons to subthreshold input currents.**
'EIF' stands for exponential integrate-and-fire; it has the same $\frac{\mathrm{d}V}{\mathrm{d}t}$ as an AdEx neuron. Adaptation currents are negligibly small for both models in this test scenario.

would. Real and AdEx neurons do not suffer this assymetry.

This nonlinearity is not visible for small voltage deviations, which is what the postsynaptic potentials we are interested in in this thesis tend to be. There is however an effect of the neuron's average voltage: if this voltage is constantly on the higher side, then inputs – both negative and positive – will cause larger responses than if the median voltage was lower.

2.4 Synapse model

One unexplained term in our neuron model, equation (1), is the synaptic current I_{syn}. This is the following sum over all input synapses i of the neuron:

$$I_{\text{syn}} = \sum_i g_i(V - E_i) \tag{15}$$

where V is the global membrane voltage of the neuron, E_i is the reversal potential of that synapse, and g_i is the local synaptic conductance, which is modulated by presynaptic spikes.

For an excitatory synapse, $V < E_i$, making $g_i(V - E_i)$ negative, increasing the membrane voltage according to the sign convention for I_{syn} in equation (1).

We simulate the synaptic conductances g_i as exponentially decaying signals (with time constant τ), and bump them up instantaneously on arrival of a presynaptic spike:

$$\frac{\mathrm{d}g_i}{\mathrm{d}t} = -g_i/\tau \tag{16}$$

On incoming presynaptic spike:

$$g_i \leftarrow g_i + \Delta g_i \tag{17}$$

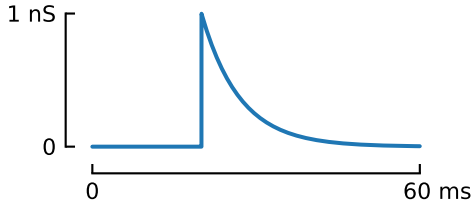

Figure 6: Example synaptic conductance trace $g_1(t)$, with a single incoming spike at $t = 20$ ms.

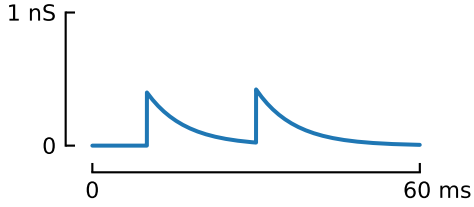

Figure 7: Another example trace $g_2(t)$, with spikes at $t = 10$ ms and 30 ms, and a smaller Δg.

Note that these are not the so called alpha-synapses. Those are two dimensional and also have an exponential rise, instead of just an exponential decay. (For an infinitely fast rise though, these models are of course the same). Simulating a full alpha synapse might increase the realism of our voltage traces, for a small simulation cost. We did not try this however. Foremost because alpha synapses fit to real data often have very fast rise times that are almost indistinguishable from instantaneous jumps.

For efficiency, we give all our excitatory synapses the same reversal potential, E_{exc}. Idem for the inhibitory synapses, with E_{inh}. This allows us to factor the synaptic current sum (equation (15)) as follows:

$$I_{\text{syn}} = (V - E_{\text{exc}}) \sum_{\text{exc } i} g_i \; + \; (V - E_{\text{inh}}) \sum_{\text{inh } i} g_i \tag{18}$$

The sums of conductance signals $g_i(t)$ can also be simplified. Say that the values of g_i at $t = 0$ are G_i. The solution to equation (16) (at least in the time until a new presynaptic spike arrives) is then

$$g_i(t) = G_i \, e^{-t/\tau} \tag{19}$$

With this, and when all synapses have the same time constant τ, the two sums in equation (18) can be factored as follows:[5]

$$\sum_i g_i(t) = \sum_i \left(G_i \, e^{-t/\tau} \right) = \left(\sum_i G_i \right) e^{-t/\tau} \tag{20}$$

[5] This is only valid in the time before any new spikes arrive. But the 'summability' still holds after a new spike. To see this, the given reasoning can be repeated, but simply with different values for the G_i (all decayed by an amount $e^{-t_{\text{spike}}/\tau}$, and one increased by a bump Δg_i), and then redefining t_{spike} to be $t = 0$.

This means that we need to only keep track of two conductance signals: g_{exc} and g_{inh}, each the sum of all excitatory or all inhibitory synaptic conductances.

Our synaptic current sum then becomes simply:

$$I_{\text{syn}} = (V - E_{\text{exc}})\, g_{\text{exc}} \; + \; (V - E_{\text{inh}})\, g_{\text{inh}}, \tag{21}$$

and we only need to simulate two differential equations, instead of one for every synapse:

$$\frac{\mathrm{d}g_{\text{exc}}}{\mathrm{d}t} = -g_{\text{exc}}/\tau$$
$$\frac{\mathrm{d}g_{\text{inh}}}{\mathrm{d}t} = -g_{\text{inh}}/\tau,$$

where on arrival of a spike at synapse i either g_{exc} or g_{inh} is instantaneously increased by a value Δg_i, depending on whether that synapse is excitatory or inhibitory.

We choose an excitatory reversal potential of $E_{\text{exc}} = 0$ mV, an inhibitory one of $E_{\text{inh}} = -80$ mV, and a time constant for the synaptic conductance decay of $\tau = 7$ ms. These values are rather arbitrary, but in line with other simulation studies (e.g. [Bre+07]).

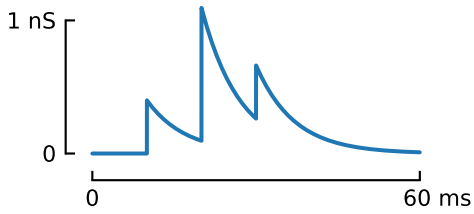

Figure 8: A third synaptic conductance trace $g_3(t)$, with three input spikes at the same times and strengths as in figures 6 and 7. This signal is simulated independently, but turns out to be equal to the sum of the two others: $g_3(t) \equiv g_1(t) + g_2(t)$.

2.5 Input spikes

In our simplest experimental setup, we simulate just one AdEx neuron. Its input is provided by an array of N Poisson neurons, i.e. they each generate spike trains according to a Poisson process. We call this the 'N-to-1' setup.

The firing rates of real neurons often follow a long-tailed distribution: most neurons do not fire much at all, while a few fire a lot. We

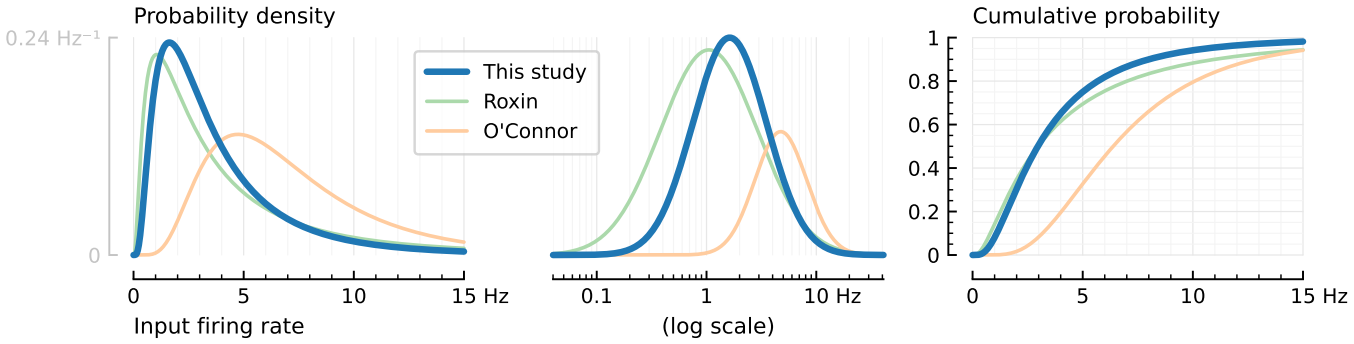

Figure 9: **Input spike trains are given log-normally distributed firing rates.**
The distribution used in our simulations is shown in bold. It has mean $\mu_x = 4$ Hz and variance of the underlying Gaussian $\sigma^2 = 0.6$. The two light distributions are from the literature. Note that the Roxin et al. distribution is slightly more heavy tailed than this study's: it has both more low firing and more high firing neurons.

recapitulate this in the firing rates of our Poisson input neurons, by drawing their firing rates from a log-normal distribution. We look to the literature for realistic parameters for this distribution, namely to the modelling paper of Roxin et al. [Rox+11], and the experimental sources it cites [HDZ08; OCo+10].

Log-normal distributions are usually parametrized with μ and σ: the location and scale of the underlying normal distribution, i.e. after log-transforming the input domain. In the above sources however, the mean μ_x of the data distribution itself is given. We can find μ, if σ is known, as $\mu = \ln(\mu_x) - \sigma^2/2$.

Roxin et al. use a mean rate μ_x of 5 Hz and a variance of the logarithm of the rate $\sigma^2 = 1.04$ in their figure 2. Hromádka et al. [HDZ08] recorded neurons in the auditory cortex of awake rats during acoustic stimulation. They find a mean firing rate μ_x of 6.2 Hz and a median of 2.4 Hz; no numeric variances are given. O'Connor et al. [OCo+10] recorded neurons in the barrel (whisker) cortex of behaving mice. Ensembled over all layers of the cortex they recorded from, they report $\mu_x = 7.4$ Hz, $\sigma_x = 12.6$ Hz, a median of 1.5 Hz, and an interquartile range of 9.5 Hz. This corresponds to a Gaussian variance of $\sigma^2 = \ln(1 + \sigma_x^2/\mu_x^2) = 0.30$. The Roxin and O'Connor distributions are also shown in figure 9.

Given these data, we choose our parameters μ and σ so that the distribution lies roughly halfway O'Connor's and Roxin's, while making sure our firing rates are rather low than high: as as our idea for connection inference rests on the number of spikes that can be used to calculate spike-triggered averages, we don't want to overestimate the number of available input spikes and obtain overly optimistic results.

Our log-normal distribution has a median of 2.96 Hz, very close to Roxin's 2.97 Hz. O'Connor's has 6.4 Hz, which is markedly different from the median of 1.5 Hz they reported (hinting that their data distribution might not be log-normal).

2.6 Voltage imaging

The signals detected by a light microscope in a voltage imaging setup are not the same as the real membrane voltage traces of which they are a reflection.

We model this lossy transformation by simply adding Gaussian noise to our simulated membrane voltage. As in the voltage imaging literature, we quantify the amount of this noise by a 'spike-SNR' measure (spike signal-to-noise ratio). This is defined as the height of an average spike relative to the standard deviation of the noise:

$$\text{spike-SNR} = \frac{\text{spike height}}{\sigma_{\text{noise}}} \tag{22}$$

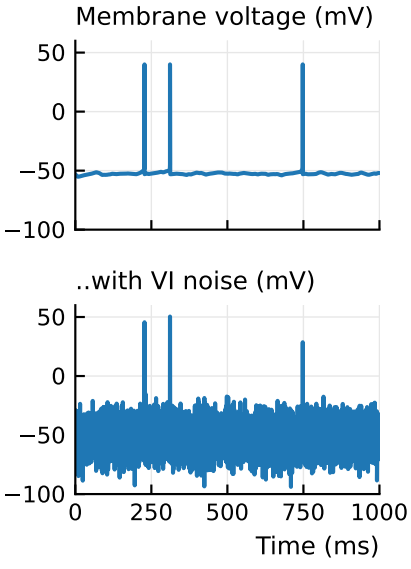

Figure 10: Simulated voltage trace (same as in figure 4, right), without and with 'voltage imaging' (VI) noise added ($\sigma_{\text{noise}} = 10.5$ mV).

In other words, if we call our output signal y, and with V_i the voltage samples resulting from the numeric integration of equation (1), we have:

$$y_i = V_i + \varepsilon_i \tag{23}$$

$$\varepsilon_i \sim \mathcal{N}(0, \sigma_{\text{noise}})$$

A typical but conservative level of noise in voltage imaging recordings has a spike-SNR of 10. If we take as spike height the spike detection threshold minus the leak potential ($\theta - E_L$, see table 2.1), we obtain a σ_{noise} of 10.5 mV.

A more realistic model of the voltage imaging-transformation would also incorporate the exponential decay over time of the SNR (with a time constant of about 10 minutes), and the short-term 'smearing in time' of voltage indicators. The latter could be done by passing the voltage signal through a linear filter with some non-instantaneous impulse response.

Chapter 3

Spike-triggered averaging

- Principle, example STAs
- Influence on STA of E/I balance, output firing rate, reversal potentials
- Use as connection test: shuffled spike trains and height of STA, p-values, and the 'area-over-start' heuristic for E vs I classification.
- Evaluation of a connection test: 'ternary' classification, summary measures, AUROC
- Performance of the simple STA-height test, for different N
- Influence of window length
- What about Vm imaging affects detection the most?

Chapter 4

New connection inference methods

4.1 STA Template correlation

- Idea for the two-pass test
- Template examples. Both ideal and template found with first-pass (STA height-only)
- Peformance for different N, & comparison with previous method

4.2 Linear regression of the upstroke

- Non-STA method: concatenated individual windows as (X, y)
- Examples of pooled windows, and fits
- Mention the problem of unknown transmission delays
- Perfomance for different N, & comparison with previous methods

4.3 Fitting a full STA model

- Model design
- Iterative model fitting
- Problem of overfitting, and parameter-constraints to solve it
- An advantage: fit parameters (like transmission delay and time constants) are biologically meaningful
- Perfomance for different N, & comparison with previous methods

4.4 Clustering, & Hierarchical model fitting

- (Time-permitting)

4.5 Zhou/Cai's 'Spike-triggered regression'

- (Time-permitting)

4.6 Computational cost

- Timings of each method, extrapolation for larger number of tested connections

4.7 Summary

- Conclusions of the N-to-1 experiment
- Leadup to the network experiments: what we could not yet test (the problem of indirect connections, as e.g. identified in the connectomics challenge)

Chapter 5

Network model

- Network connectivity, E/I balance, raster plots
- Too many possible connections to test them all → Subsampling
- Performance of last chapter's methods
- If time: experiment with a network that is less densely connected than our current fully-random one. Why? To better examine the effect of indirect connections / colliders (For the current connectivity, there are too many of those. But in a more realistic, 'localized' network, there are less, and so it seems easier to isolate and examine their effect).

Chapter 6

Discussion

6.1 Summary & conclusions

..

6.2 Future work

- Test on real data
- Direct comparison with spikes-only methods
- More complexity in the testing setup: different transmission delays and time constants per synapse / neuron, plus:
- Short term synaptic plasticity. Bursting. Oscillations.
- Simulate different brain areas (different cell types and connectivity patterns). Simulate the same area, but in different states (up vs down, e.g.)
- New connection test method to try: something deep learning-based (we have infinite training data, given our simulation)

References

[Bad+08] Laurent Badel, Sandrine Lefort, Thomas K. Berger, Carl C. H. Petersen, Wulfram Gerstner, and Magnus J. E. Richardson. "Extracting Non-Linear Integrate-and-Fire Models from Experimental Data Using Dynamic I−V Curves". In: *Biological Cybernetics* (Nov. 15, 2008). DOI: 10.1007/s00422-008-0259-4.

[BG05] Romain Brette and Wulfram Gerstner. "Adaptive Exponential Integrate-and-Fire Model as an Effective Description of Neuronal Activity". In: *Journal of Neurophysiology* (Nov. 2005). DOI: 10.1152/jn.00686.2005.

[Bre+07] Romain Brette et al. "Simulation of Networks of Spiking Neurons: A Review of Tools and Strategies". In: *Journal of Computational Neuroscience* (Dec. 1, 2007). DOI: 10.1007/s10827-007-0038-6.

[DA01] Peter Dayan and L. F. Abbott. *Theoretical Neuroscience: Computational and Mathematical Modeling of Neural Systems*. Computational Neuroscience. The MIT Press, 2001. 460 pp. ISBN: 978-0-262-04199-7.

[HDZ08] Tomáš Hromádka, Michael R. DeWeese, and Anthony M. Zador. "Sparse Representation of Sounds in the Unanesthetized Auditory Cortex". In: *PLOS Biology* (Jan. 29, 2008). DOI: 10.1371/journal.pbio.0060016.

[Izh07] Eugene M. Izhikevich. *Dynamical Systems in Neuroscience: The Geometry of Excitability and Bursting*. Cambridge, Mass.: The MIT Press, 2007. 464 pp. ISBN: 978-0-262-51420-0.

[Nau+08] Richard Naud, Nicolas Marcille, Claudia Clopath, and Wulfram Gerstner. "Firing Patterns in the Adaptive Exponential Integrate-and-Fire Model". In: *Biological Cybernetics* (Nov. 15, 2008). DOI: 10.1007/s00422-008-0264-7.

[OCo+10] Daniel H. O'Connor, Simon P. Peron, Daniel Huber, and Karel Svoboda. "Neural Activity in Barrel Cortex Underlying Vibrissa-Based Object Localization in Mice". In: *Neuron* (Sept. 23, 2010). DOI: 10.1016/j.neuron.2010.08.026. pmid: 20869600.

[Rox+11] Alex Roxin, Nicolas Brunel, David Hansel, Gianluigi Mongillo, and Carl van Vreeswijk. "On the Distribution of Firing Rates in Networks of Cortical Neurons". In: *Journal of Neuroscience* (Nov. 9, 2011). DOI: 10.1523/JNEUROSCI.1677-11.2011. pmid: 22072673.